

Structural Studies on Monohalogenated Derivatives of the Phytohormone Indole-3-acetic Acid (Auxin)[†]

BILJANA NIGOVIĆ,^a BISERKA KOJIĆ-PRODIĆ,^{a*} SNJEŽANA ANTOLIĆ,^a SANJA TOMIĆ,^a VITOMIR PUNTAREC^a AND JERRY D. COHEN^b

^aRuder Bošković Institute, PO Box 1016, 10001 Zagreb, Croatia, and ^bHorticultural Crops Quality Laboratory, Beltsville Agricultural Research Center, USDA/ARS Beltsville, MD 20705, USA

(Received 18 April 1995; accepted 22 June 1995)

Abstract

The physiological properties of the phytohormone (auxin) indole-3-acetic acid (IAA) and its ring substituted derivatives have so far been rationalized by a number of contradictory hypotheses based on incomplete structural data deduced mainly by inspection of molecular models. In order to give more evidence for structure–activity relationships of monohalogenated IAA's, the molecular structures of the natural auxin 4-Cl-IAA as well as 5-Cl-IAA, 6-Cl-IAA, 7-Cl-IAA and 5-Br-IAA have been compared, as revealed by X-ray analysis, and molecular mechanics and dynamics. The influence of the substitution site and the size of the halogen atom and bioactivity is discussed. The typical structural feature of the molecules studied is the slight distortion of part of the indole nucleus around C7: bond length C6–C7 1.368(6) Å and C6–C7–C71 117.6(3)° (average values of five structures and seven molecules). The conformations of monohalogenated indole-3-acetic acid molecules, characteristic for auxins, are defined by rotations about two bonds only: one describes the relative orientation of a side chain towards the indole moiety and the second the orientation of the carboxylic group. The results of X-ray structure analysis, and molecular mechanics and dynamics revealed the folded shape of the molecules in all compounds studied. *Ab initio* calculations showed that the planar conformation can be adopted as well. Crystal data at 297 K for 4-Cl-IAA, 6-Cl-IAA, 7-Cl-IAA and 5-Br-IAA, and at 220 K for 5-Cl-IAA, using Mo *K*α radiation ($\lambda = 0.71073$ Å), and Cu *K*α ($\lambda = 1.5418$ Å) for 6-Cl-IAA, are as follows: 4-Cl-IAA, C₁₀H₈ClNO₂, $M_r = 209.63$, monoclinic, $P2_1/c$, $a = 7.313(4)$, $b = 17.156(4)$, $c = 7.640(4)$ Å, $\beta = 92.71(5)^\circ$, $V = 957.5(1)$ Å³, $Z = 4$, $D_x = 1.454$ g cm⁻³, $\mu = 3.7$ cm⁻¹, $F(000) = 432$, $R = 0.037$, $wR = 0.039$ for 1040 symmetry-independent [$I \geq 3\sigma(I)$] reflections; 5-Cl-IAA, C₁₀H₈ClNO₂, monoclinic, $P2_1/c$, $a = 19.141(4)$, $b = 5.154(2)$, $c = 10.323(3)$ Å, $\beta = 116.23(2)^\circ$, $V = 913.5(1)$ Å³, $Z = 4$, $D_x =$

1.524 g cm⁻³, $\mu = 3.8$ cm⁻¹, $F(000) = 432$, $R = 0.039$, $wR = 0.042$ for 1184 symmetry-independent [$I \geq 3\sigma(I)$] reflections; 6-Cl-IAA, C₁₀H₈ClNO₂, orthorhombic, $Pbca$, $a = 61.08(1)$, $b = 12.115(7)$, $c = 7.674(5)$ Å, $V = 5679(5)$ Å³, $Z = 24$, $D_x = 1.471$ g cm⁻³, $\mu = 33.9$ cm⁻¹, $F(000) = 2592$, $R = 0.052$, $wR = 0.052$ for 3030 symmetry-independent [$I \geq \sigma(I)$] reflections; 7-Cl-IAA, C₁₀H₈ClNO₂, monoclinic, $P2_1/c$, $a = 20.244(5)$, $b = 4.829(2)$, $c = 10.728(4)$ Å, $\beta = 116.30(1)^\circ$, $V = 940(1)$ Å³, $Z = 4$, $D_x = 1.481$ g cm⁻³, $\mu = 3.7$ cm⁻¹, $F(000) = 432$, $R = 0.042$, $wR = 0.029$ for 889 symmetry-independent [$I \geq 3\sigma(I)$] reflections; 5-Br-IAA, C₁₀H₈BrNO₂, $M_r = 254.08$, triclinic, $P\bar{1}$, $a = 5.645(3)$, $b = 9.713(4)$, $c = 10.019(4)$ Å, $\alpha = 116.02(3)$, $\beta = 92.67(5)$, $\gamma = 100.12(4)^\circ$, $V = 481.2(5)$ Å³, $Z = 2$, $D_x = 1.754$ g cm⁻³, $\mu = 42.0$ cm⁻¹, $F(000) = 252$, $R = 0.029$, $wR = 0.020$ for 1865 symmetry-independent [$I \geq 3\sigma(I)$] reflections.

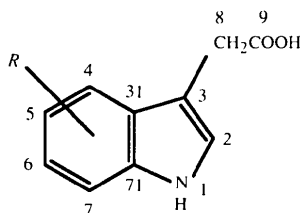
1. Introduction

Certain chloro-substituted indole-3-acetic acids with auxin activity occur in nature: 4-Cl-IAA and its methyl ester are found in *Pisum sativum*, *Vicia faba* and *Lathyrus latifolius* (Marumo, Abe, Hattori & Munakata, 1968; Marumo, Hattori, Abe & Munakata, 1968; Marumo, Hattori & Abe, 1971; Engvild, Egsgaard & Larsen, 1978; Hofinger & Böttger, 1979). 4-Cl-IAA was reported to also be present in seeds of *Pinus sylvestris* (Ernstsen & Sandberg, 1986). 4-Cl-IAA and 6-Cl-IAA are more effective than IAA in stimulating *Avena coleoptile* straight growth (Böttger, Engvild & Soll, 1978) or pea stem elongation (Katekar & Geissler, 1982, 1983). 5-Cl-IAA is of moderate activity, whereas 5-Br-IAA is less active (Böttger, Engvild & Soll, 1978). However, 7-Cl-IAA shows anti-auxin activity (Stenlid & Engvild; 1987). The role of 4-Cl-IAA in the plant is not clear and little is known about its metabolism or the possibility to replace IAA. Very close structural similarity of the chloro-substituted IAA's to IAA might reveal some competitive antagonists to IAA as well.

The halogenated species of IAA are more lipophilic in nature than IAA and thus they can be easily transported through membranes. On the basis of very pro-

[†] The authors dedicate the title paper to the 65th anniversary of Professor Dr Dieter Klämbt, Rheinische Friedrich-Wilhelms Universität, Bonn, who has contributed a great deal to the molecular biology of the auxins.

nounced auxin activity of halogenated IAA's, compared with the hormone itself, direct correlation between the auxin activity and the lipophilicity could be expected. However, dihalogenated indole-3-acetic acids, which are more lipophilic than monohalogenated species, show auxin antagonism; more probably they bind to a different receptor. Hormone activity is a very complex mechanism influenced by many steric and physicochemical parameters. A direct answer to the problem could be possible by determining the three-dimensional structure of the receptor + hormone complex along kinetics of the active site changes. The lack of such knowledge leaves the option of studying the molecular properties of auxin agonists and antagonists. The comparative molecular field analysis (CoMFA; Cramer, Scott, DePriest, Patterson & Hecht, 1993) as one of the 3D QSAR approaches applied to agonists and antagonists could offer information on the enzymatic properties at the active site. The structural studies of monohalogenated IAA's listed in Scheme I are aimed at recognizing the typical structural features of auxin(s).



4-Cl-IAA, 5-Cl-IAA, 6-Cl-IAA, 7-Cl-IAA

$R = \text{Cl}$

5-Br-IAA

$R = \text{Br}$

Scheme I. Structural formulae of monohalogenated indole-3-acetic acids and their abbreviations used.

2. X-ray analysis

5-Br-IAA was obtained from Aldrich, whereas 4-Cl-IAA, 5-Cl-IAA, 6-Cl-IAA and 7-Cl-IAA were synthesized from the halogenated phenylhydrazones (Aldrich), as described by Baldi, Slovin & Cohen (1985). The crystals suitable for X-ray structure analysis were prepared by slow evaporation of 2 ml solutions containing 10–15 mg ml⁻¹ of compounds in solvent mixtures: methanol + water (1:1, vol.) for 6-Cl-IAA, methanol + 2-propanol + water (1:1:1, vol.) for 7-Cl-IAA, ethyl acetate

+ benzene (1:1, vol.) for 4-Cl-IAA and 5-Cl-IAA, and for 5-Br-IAA ethyl acetate + *n*-hexane (1:1, vol.). The crystals were grown at room temperature over a few days.

The compounds studied have no chiral centers and accordingly crystallize in the centrosymmetric space groups $P2_1/c$, $Pbca$ (a single case) and $P\bar{1}$ (a single case). Data were collected on the Enraf–Nonius CAD-4 diffractometer (Table 1) with graphite-monochromated Mo $K\alpha$ and Cu $K\alpha$ (for 6-Cl-IAA) radiation and rescaled for decay on the basis of intensity reduction of standard reflections; the maximum reduction was 2.7% for 7-Cl-IAA. Lorentz and polarization corrections were applied using an Enraf–Nonius SDP package (B. A. Frenz & Associates, Inc., 1982). Structures were solved by direct methods using the program SHELXS86 (Sheldrick, 1985) and refined by SHELX76 (Sheldrick, 1976) with a full-matrix least-squares procedure minimizing $w(|F_o| - |F_c|)^2$ on F values. Difference-Fourier maps were used to locate the H atoms. In the structures of 4-, 5-, 6- and 7-Cl-IAA's the indole N—H bond distances were normalized to the values obtained by neutron diffraction (N—H 1.009 Å). The O—H distances in all the structures studied were also normalized. The non-H atoms were refined anisotropically; details of the refinement procedures are listed in Table 1. Scattering factors are those included in SHELX76 (Sheldrick, 1976). Molecular geometry was calculated by the program package EUCLID (Spek, 1982). Drawings were prepared by the PLUTON program incorporated into EUCLID and ORTEPII (Johnson, 1976). The final atomic coordinates and equivalent isotropic thermal parameters are listed in Table 2.* Calculations were performed on MicroVAXII and INDIGO-2 computers of the X-ray Laboratory, Rudjer Bošković, Zagreb, Croatia.

3. Molecular structures in the crystalline state

Interatomic distances, bond and selected torsion angles for monohalogenated indole-3-acetic acids are listed in Tables 3, 4 and 5. The molecular structures

* Lists of atomic coordinates, anisotropic displacement parameters and structure factors have been deposited with the IUCr (Reference: SE0178). Copies may be obtained through The Managing Editor, International Union of Crystallography, 5 Abbey Square, Chester CH1 2HU, England.

Table 1. *Experimental details*

	4-Cl-IAA	5-Cl-IAA	6-Cl-IAA	7-Cl-IAA	5-Br-IAA
Crystal data					
Chemical formula	C ₁₀ H ₈ ClNO ₂	C ₁₀ H ₈ ClNO ₂	C ₁₀ H ₈ ClNO ₂	C ₁₀ H ₈ ClNO ₂	C ₁₀ H ₈ BrNO ₂
Chemical formula weight	209.63	209.63	209.63	209.63	254.08
Cell setting	Monoclinic	Monoclinic	Orthorhombic	Monoclinic	Triclinic
Space group	$P2_1/c$	$P2_1/c$	$Pbca$	$P2_1/c$	$P\bar{1}$
<i>a</i> (Å)	7.313 (4)	19.141 (4)	61.08 (1)	20.244 (5)	5.645 (3)
<i>b</i> (Å)	17.156 (4)	5.154 (2)	12.115 (7)	4.829 (2)	9.713 (4)
<i>c</i> (Å)	7.640 (4)	10.323 (3)	7.674 (5)	10.728 (4)	10.019 (4)

Table 1 (cont.)

	4-Cl-IAA	5-Cl-IAA	6-Cl-IAA	7-Cl-IAA	5-Br-IAA
α ($^\circ$)	90.0	90.0	90.0	90.0	116.02 (3)
β ($^\circ$)	92.71 (5)	116.23 (2)	90.0	116.30 (1)	92.67 (5)
γ ($^\circ$)	90.0	90.0	90.0	90.0	100.12 (4)
V (\AA^3)	957.5 (1)	913.5 (1)	5679 (5)	940 (1)	481.2 (5)
Z	4	4	24	4	2
D_x (Mg m^{-3})	1.454	1.524	1.471	1.481	1.754
Radiation type	Mo $K\alpha$	Mo $K\alpha$	Cu $K\alpha$	Mo $K\alpha$	Mo $K\alpha$
Wavelength (\AA)	0.71073	0.71073	1.54184	0.71073	0.71073
No. of reflections for cell parameters	25	25	25	25	25
θ range ($^\circ$)	6–19	9–18	15–47	6–20	6–17
μ (mm^{-1})	0.37	0.38	3.39	0.37	4.20
Temperature (K)	297	220	295	297	297
Crystal form	Plate	Prismatic	Plate	Prismatic	Prismatic
Crystal size (mm)	0.34 \times 0.28 \times 0.08	0.30 \times 0.25 \times 0.15	0.40 \times 0.14 \times 0.04	0.50 \times 0.30 \times 0.10	0.40 \times 0.30 \times 0.20
Data collection					
Diffractometer	Enraf–Nonius CAD-4	Enraf–Nonius CAD-4	Enraf–Nonius CAD-4	Enraf–Nonius CAD-4	Enraf–Nonius CAD-4
Data collection method	ω - 2θ	ω - 2θ	ω - 2θ	ω - 2θ	ω - 2θ
Absorption correction	None	None	None	None	ψ scan
T_{\min}	—	—	—	—	0.85
T_{\max}	—	—	—	—	1.00
No. of measured reflections	2364	1912	6199	2682	5750
No. of independent reflections	1040	1184	3030	889	2659
No. of observed reflections	1040	1184	3030	889	1865
Criterion for observed reflections	$I > 3\sigma(I)$	$I > 3\sigma(I)$	$I > \sigma(I)$	$I > 3\sigma(I)$	$I > 3\sigma(I)$
R_{int}	0.059	0.037	0.038	0.034	0.048
θ_{max} ($^\circ$)	25	25	70	25	30
Range of h, k, l	0 \rightarrow h \rightarrow 8 -1 \rightarrow k \rightarrow 20 -9 \rightarrow l \rightarrow 9	0 \rightarrow h \rightarrow 12 0 \rightarrow k \rightarrow 6 -20 \rightarrow l \rightarrow 20	0 \rightarrow h \rightarrow 9 0 \rightarrow k \rightarrow 14 0 \rightarrow l \rightarrow 74	-1 \rightarrow h \rightarrow 12 -1 \rightarrow k \rightarrow 5 -21 \rightarrow l \rightarrow 21	-7 \rightarrow h \rightarrow 7 -13 \rightarrow k \rightarrow 13 -14 \rightarrow l \rightarrow 14
No. of standard reflections	3	3	3	3	3
Frequency of standard reflections	Every 3 h	Every 3 h	Every 3 h	Every 3 h	Every 3 h
Intensity decay (%)	0.8	0.7	2.5	2.7	1.5
Refinement					
Refinement on	F	F	F	F	F
R	0.037	0.039	0.052	0.042	0.029
wR	0.039	0.042	0.052	0.029	0.020
S	0.58	0.61	1.98	0.61	0.39
No. of reflections used in refinement	1467	1120	3030	889	2659
No. of parameters used	159	161	154	159	159
H-atom treatment	All H-atom parameters refined; N—H, OH normalized	All H-atom parameters refined; N—H, OH normalized	All H-atom parameters refined; N—H, OH normalized	All H-atom parameters refined; N—H, OH normalized	All H-atom parameters refined; N—H, OH normalized
Weighting scheme	$w = k[\sigma^2(F_o) + g(F_o)^2]$	$w = k[\sigma^2(F_o) + g(F_o)^2]$	$w = k[\sigma^2(F_o) + g(F_o)^2]$	$w = k[\sigma^2(F_o) + g(F_o)^2]$	$w = k[\sigma^2(F_o) + g(F_o)^2]$
g	0.000392	0.00071	0.00021	0.0	0.0
$(\Delta/\sigma)_{\text{max}}$	0.009	0.017	0.132	0.170	0.109
$\Delta\rho_{\text{max}}$ ($\text{e } \text{\AA}^{-3}$)	0.21	0.29	0.25	0.20	0.45
$\Delta\rho_{\text{min}}$ ($\text{e } \text{\AA}^{-3}$)	-0.25	-0.27	-0.24	-0.20	-0.42
Extinction method	None	None	None	None	None
Source of atomic scattering factors	SHELX76 (Sheldrick, 1976)	SHELX76 (Sheldrick, 1976)	SHELX76 (Sheldrick, 1976)	SHELX76 (Sheldrick, 1976)	SHELX76 (Sheldrick, 1976)
Computer programs					
Data collection	CAD-4 (Enraf–Nonius, 1989)	CAD-4 (Enraf–Nonius, 1989)	CAD-4 (Enraf–Nonius, 1989)	CAD-4 (Enraf–Nonius, 1989)	CAD-4 (Enraf–Nonius, 1989)
Cell refinement	CAD-4 (Enraf–Nonius, 1989)	CAD-4 (Enraf–Nonius, 1989)	CAD-4 (Enraf–Nonius, 1989)	CAD-4 (Enraf–Nonius, 1989)	CAD-4 (Enraf–Nonius, 1989)
Data reduction	SDP (B. A. Frenz & Associates, Inc., 1982)	SDP (B. A. Frenz & Associates, Inc., 1982)	SDP (B. A. Frenz & Associates, Inc., 1982)	SDP (B. A. Frenz & Associates, Inc., 1982)	SDP (B. A. Frenz & Associates, Inc., 1982)
Structure solution	SHELXS86 (Sheldrick, 1985)	SHELXS86 (Sheldrick, 1985)	SHELXS86 (Sheldrick, 1985)	SHELXS86 (Sheldrick, 1985)	SHELXS86 (Sheldrick, 1985)
Structure refinement	SHELX76 (Sheldrick, 1976)	SHELX76 (Sheldrick, 1976)	SHELX76 (Sheldrick, 1976)	SHELX76 (Sheldrick, 1976)	SHELX76 (Sheldrick, 1976)
Preparation of material for publication	PLATON (Spek, 1990) and WORD5	PLATON (Spek, 1990) and WORD5	PLATON (Spek, 1990) and WORD5	PLATON (Spek, 1990) and WORD5	PLATON (Spek, 1990) and WORD5

Table 2. Fractional atomic coordinates and equivalent isotropic displacement parameters (Å²)
$$U_{\text{eq}} = (1/3) \sum_i \sum_j U_{ij} a_i^* a_j^* \mathbf{a}_i \cdot \mathbf{a}_j.$$

	x	y	z	U_{eq}
4-Cl-IAA				
Cl	0.8897 (1)	0.0550 (1)	0.7828 (1)	0.0754 (4)
O1	1.4303 (3)	-0.0344 (1)	0.7799 (3)	0.0591 (9)
O2	1.3956 (3)	0.0775 (1)	0.9195 (2)	0.0469 (7)
N1	1.2461 (4)	0.2797 (2)	0.5781 (3)	0.057 (1)
C2	1.3375 (5)	0.2119 (2)	0.5553 (4)	0.056 (1)
C3	1.2395 (4)	0.1509 (2)	0.6137 (3)	0.045 (1)
C31	1.0726 (4)	0.1830 (2)	0.6729 (3)	0.0378 (9)
C4	0.9126 (4)	0.1548 (2)	0.7429 (3)	0.046 (1)
C5	0.7730 (5)	0.2035 (2)	0.7845 (4)	0.056 (1)
C6	0.7902 (5)	0.2833 (2)	0.7609 (4)	0.062 (1)
C7	0.9427 (5)	0.3146 (2)	0.6941 (4)	0.056 (1)
C71	1.0815 (4)	0.2642 (2)	0.6488 (3)	0.044 (1)
C8	1.3028 (6)	0.0682 (2)	0.6134 (4)	0.056 (1)
C9	1.3783 (4)	0.0387 (2)	0.7865 (3)	0.0408 (9)
5-Cl-IAA				
Cl	0.41963 (4)	0.7884 (2)	0.39347 (8)	0.0478 (3)
O1	0.0157 (1)	0.7957 (5)	-0.0860 (3)	0.0562 (9)
O2	0.0773 (1)	0.4200 (5)	-0.0197 (3)	0.0545 (9)
N1	0.2572 (1)	0.2417 (6)	-0.1507 (3)	0.0454 (9)
C2	0.1891 (2)	0.3795 (6)	-0.2103 (4)	0.042 (1)
C3	0.1883 (2)	0.5618 (6)	-0.1167 (3)	0.0342 (9)
C31	0.2618 (1)	0.5417 (5)	0.0100 (3)	0.0299 (8)
C4	0.2977 (2)	0.6825 (5)	0.1378 (3)	0.0325 (9)
C5	0.3720 (2)	0.6129 (5)	0.2341 (3)	0.0354 (9)
C6	0.4115 (2)	0.4044 (6)	0.2099 (4)	0.039 (1)
C7	0.3774 (2)	0.2662 (6)	0.0850 (4)	0.042 (1)
C71	0.3030 (2)	0.3374 (5)	-0.0155 (3)	0.0359 (9)
C8	0.1222 (2)	0.7361 (7)	-0.1373 (4)	0.038 (1)
C9	0.0708 (1)	0.6324 (6)	-0.0739 (3)	0.0341 (9)
6-Cl-IAA, molecule A				
Cl1	0.13761 (2)	0.1729 (1)	0.1730 (1)	0.0801 (4)
O1	-0.00095 (4)	-0.0513 (2)	0.2189 (3)	0.0595 (9)
O2	0.02213 (4)	0.0620 (2)	0.0819 (3)	0.062 (1)
N1	0.06258 (6)	0.2604 (3)	0.4579 (4)	0.063 (1)
C2	0.04363 (7)	0.2015 (4)	0.4704 (5)	0.063 (2)
C3	0.04608 (6)	0.1023 (3)	0.3924 (5)	0.054 (1)
C4	0.08025 (7)	0.0192 (3)	0.2356 (5)	0.056 (1)
C5	0.10149 (7)	0.0431 (3)	0.1915 (5)	0.060 (1)
C6	0.11086 (6)	0.1445 (3)	0.2378 (5)	0.058 (1)
C7	0.09935 (6)	0.2235 (3)	0.3288 (5)	0.055 (1)
C8	0.02881 (7)	0.0137 (4)	0.3798 (5)	0.065 (2)
C9	0.01646 (6)	0.0115 (3)	0.2123 (5)	0.051 (1)
C31	0.06790 (6)	0.0976 (3)	0.3276 (4)	0.049 (1)
C71	0.07784 (6)	0.1993 (3)	0.3719 (4)	0.051 (1)
6-Cl-IAA, molecule B				
Cl11	0.03035 (2)	0.70559 (9)	0.4247 (1)	0.0813 (5)
O11	0.16498 (4)	0.4319 (2)	0.0358 (3)	0.064 (1)
O21	0.14653 (4)	0.5778 (2)	-0.0603 (3)	0.067 (1)
N11	0.11491 (5)	0.7377 (3)	0.3941 (4)	0.060 (1)
C21	0.13060 (7)	0.6683 (4)	0.3290 (5)	0.062 (2)
C41	0.07973 (6)	0.5261 (3)	0.2395 (4)	0.046 (1)
C51	0.05939 (6)	0.5621 (3)	0.2836 (5)	0.052 (1)
C61	0.05666 (6)	0.6631 (3)	0.3695 (5)	0.052 (1)
C81	0.13258 (6)	0.4775 (3)	0.1827 (5)	0.059 (1)
C91	0.14862 (6)	0.5021 (3)	0.0422 (5)	0.052 (1)
C310	0.12114 (6)	0.5766 (3)	0.2592 (5)	0.049 (1)
C311	0.09818 (5)	0.5905 (3)	0.2801 (4)	0.041 (1)
C710	0.07410 (6)	0.7298 (3)	0.4137 (5)	0.052 (1)
C711	0.09473 (6)	0.6925 (3)	0.3672 (4)	0.047 (1)
6-Cl-IAA, molecule C				
Cl12	0.30106 (2)	0.3132 (1)	0.5015 (2)	0.0892 (5)
O12	0.16735 (5)	0.5845 (2)	0.6354 (4)	0.071 (1)
O22	0.18824 (4)	0.4501 (2)	0.7427 (3)	0.0625 (9)
N12	0.22057 (6)	0.2482 (3)	0.3122 (5)	0.069 (1)
C22	0.20195 (8)	0.3120 (3)	0.3266 (6)	0.070 (2)
C32	0.20692 (7)	0.4082 (3)	0.4085 (5)	0.059 (1)
C42	0.24469 (7)	0.4769 (3)	0.5286 (5)	0.058 (1)
C52	0.26639 (8)	0.4489 (3)	0.5409 (5)	0.063 (1)

Table 2 (cont.)

	x	y	z	U_{eq}
C62	0.27358 (7)	0.3469 (3)	0.4747 (5)	0.061 (1)
C72	0.25983 (7)	0.2741 (3)	0.3944 (5)	0.058 (1)
C82	0.19166 (8)	0.5029 (4)	0.4422 (5)	0.071 (2)
C92	0.18253 (6)	0.5083 (3)	0.6213 (5)	0.052 (1)
C312	0.22991 (6)	0.4049 (3)	0.4476 (4)	0.049 (1)
C712	0.23796 (7)	0.3029 (3)	0.3825 (5)	0.052 (1)
7-Cl-IAA				
Cl	0.4362	0.6484 (2)	0.6135 (1)	0.0876 (4)
O1	0.0074 (2)	1.2522 (6)	0.1275 (3)	0.090 (1)
O2	0.0796 (1)	0.9060 (6)	0.1306 (2)	0.086 (1)
N1	0.2696 (2)	0.7463 (7)	0.5524 (3)	0.064 (2)
C2	0.1983 (2)	0.8362 (9)	0.5065 (4)	0.062 (2)
C3	0.1831 (2)	1.0309 (7)	0.4074 (4)	0.058 (1)
C31	0.2481 (2)	1.0651 (7)	0.3890 (3)	0.055 (2)
C4	0.2679 (2)	1.2329 (8)	0.3055 (4)	0.069 (2)
C5	0.3372 (3)	1.2140 (9)	0.3154 (4)	0.077 (2)
C6	0.3894 (2)	1.0317 (9)	0.4074 (4)	0.073 (2)
C7	0.3722 (2)	0.8671 (8)	0.4924 (3)	0.062 (2)
C71	0.3018 (2)	0.8821 (7)	0.4823 (3)	0.055 (2)
C8	0.1136 (2)	1.189 (1)	0.3354 (4)	0.070 (2)
C9	0.0663 (2)	1.0986 (9)	0.1869 (4)	0.062 (2)
5-Br-IAA				
Br	0.00865 (4)	0.21409 (3)	0.44576 (3)	0.0590 (1)
O1	-0.2627 (2)	0.9724 (1)	0.8741 (2)	0.0579 (4)
O2	-0.1475 (2)	0.8191 (1)	0.9642 (1)	0.0493 (3)
N1	-0.7224 (3)	0.3900 (2)	0.8680 (2)	0.0513 (4)
C2	-0.7263 (3)	0.5356 (2)	0.8808 (2)	0.0511 (4)
C3	-0.5668 (3)	0.5755 (2)	0.8008 (2)	0.0393 (4)
C31	-0.4522 (3)	0.4447 (2)	0.7312 (2)	0.0365 (4)
C4	-0.2806 (3)	0.4112 (2)	0.6315 (2)	0.0387 (4)
C5	-0.2172 (3)	0.2694 (2)	0.5860 (2)	0.0409 (4)
C6	-0.3082 (4)	0.1606 (2)	0.6359 (2)	0.0495 (4)
C7	-0.4798 (4)	0.1910 (2)	0.7325 (2)	0.0498 (4)
C71	-0.5518 (3)	0.3325 (2)	0.7774 (2)	0.0411 (4)
C8	-0.5170 (3)	0.7246 (2)	0.7896 (2)	0.0445 (4)
C9	-0.2917 (3)	0.8413 (2)	0.8854 (2)	0.0384 (4)

are shown in Fig. 1. Bond distances and angles in the monohalogenated indole-3-acetic acids have been influenced by various substituents (Cl and Br) attached at the 4-, 5-, 6- and 7- positions of the phenyl ring. The shortening of the C4—C5 bond [$<1.365(6) \text{ \AA}>$] is comparable to those in free IAA [$1.376(5) \text{ \AA}$ (Chandrasekhar & Raghunathan, 1982)] and *n*-alkylated indole-3-acetic acids [$<1.378(6) \text{ \AA}$ (Kojić-Prodić, Nigović, Tomić *et al.*, 1991)] observed earlier. In 4-Cl-IAA the closing of the C4—C31—C71 angle to the value of $116.0(3)^\circ$ is affected by substitution at position 4 of the phenyl moiety. The opening of the C4—C5—C6 angle is pronounced for compounds with substituents at position 5 [Table 4; *e.g.* $122.7(3)^\circ$ for 5-Cl-IAA and $123.8(2)^\circ$ for 5-Br-IAA]. However, correlation between the angle opening and the size or polarizability of the substituted halogen atoms cannot be found. Contraction of the C6—C7 bond [$<1.368(6) \text{ \AA}>$, mean value for the five structures presented in Table 3], closing of the C6—C7—C71 angle [$<117.9(3)^\circ>$, Table 4] and opening of the C31—C71—C7 angle [$<122.5(3)^\circ>$] were observed in the phenyl ring of the indole moiety. This distortion of the phenyl ring of the indole nucleus was found in low- and room-temperature diffraction data for IAA

Table 3. Bond lengths (Å) for monohalogenated indole-3-acetic acids

	4-Cl-IAA	5-Cl-IAA	6-Cl-IAA	7-Cl-IAA	5-Br-IAA
			A	B	C
N1—C2	1.357 (5)	1.369 (5)	1.363 (6)	1.369 (6)	1.380 (6)
N1—C71	1.369 (4)	1.370 (4)	1.361 (5)	1.364 (5)	1.363 (6)
C2—C3	1.356 (5)	1.353 (5)	1.351 (6)	1.362 (6)	1.358 (5)
C3—C31	1.432 (4)	1.440 (4)	1.424 (5)	1.422 (5)	1.436 (6)
C4—C31	1.396 (4)	1.392 (4)	1.403 (5)	1.406 (5)	1.401 (5)
C4—C5	1.368 (5)	1.375 (5)	1.372 (6)	1.359 (9)	1.371 (6)
C5—C6	1.387 (5)	1.398 (5)	1.401 (5)	1.400 (5)	1.406 (5)
C6—C7	1.359 (5)	1.361 (5)	1.378 (5)	1.379 (5)	1.365 (6)
C7—C71	1.390 (5)	1.390 (5)	1.386 (5)	1.385 (5)	1.384 (6)
C31—C71	1.407 (5)	1.408 (4)	1.415 (5)	1.421 (5)	1.421 (5)
C3—C8	1.492 (5)	1.488 (5)	1.508 (6)	1.508 (5)	1.501 (6)
C8—C9	1.497 (4)	1.500 (5)	1.491 (6)	1.487 (5)	1.485 (6)
O1—C9	1.312 (4)	1.311 (4)	1.309 (4)	1.313 (4)	1.313 (5)
O2—C9	1.216 (3)	1.211 (4)	1.223 (5)	1.215 (4)	1.219 (5)
Cl—C4	1.749 (4)				1.203 (5)
Cl—C5		1.741 (3)			
Cl—C6			1.742 (4)	1.740 (4)	1.740 (5)
Cl—C7					1.729 (4)
Br—C5					1.906 (2)

Table 4. Bond angles (°) for monohalogenated indole-3-acetic acids

	4-Cl-IAA	5-Cl-IAA	6-Cl-IAA	7-Cl-IAA	5-Br-IAA
			A	B	C
C2—N1—C71	109.4 (3)	108.9 (3)	109.3 (3)	109.3 (3)	109.8 (3)
N1—C2—C3	110.4 (3)	110.4 (3)	109.9 (4)	110.3 (4)	109.5 (4)
C2—C3—C8	124.4 (3)	126.5 (3)	125.7 (4)	127.3 (3)	126.6 (4)
C2—C3—C31	106.2 (3)	106.5 (3)	107.1 (3)	106.1 (3)	106.9 (4)
C31—C3—C8	129.4 (3)	126.9 (3)	127.2 (3)	126.5 (3)	126.3 (4)
C3—C31—C4	136.9 (3)	134.3 (3)	134.9 (4)	134.4 (3)	134.9 (3)
C3—C31—C71	107.1 (3)	106.7 (3)	106.4 (3)	107.6 (3)	106.8 (3)
C4—C31—C71	116.0 (3)	119.0 (3)	118.7 (3)	117.9 (3)	118.3 (3)
C31—C4—C5	121.7 (3)	118.0 (3)	119.3 (3)	120.0 (3)	120.0 (3)
C4—C5—C6	119.9 (3)	122.7 (3)	120.6 (4)	120.4 (3)	119.6 (4)
C5—C6—C7	121.3 (3)	120.0 (3)	122.0 (4)	122.4 (3)	122.6 (4)
C6—C7—C71	118.0 (3)	118.2 (3)	117.2 (3)	116.6 (3)	117.4 (4)
C31—C71—C7	123.0 (3)	122.1 (3)	122.2 (3)	122.7 (3)	122.0 (4)
N1—C71—C7	130.1 (3)	130.4 (3)	130.5 (3)	130.7 (3)	131.0 (4)
N1—C71—C31	106.9 (3)	107.5 (3)	107.2 (3)	106.6 (3)	107.0 (3)
C3—C8—C9	114.9 (3)	113.7 (3)	115.0 (3)	115.3 (3)	115.2 (3)
C8—C9—O1	112.6 (2)	112.6 (3)	112.8 (3)	113.5 (3)	111.9 (3)
C8—C9—O2	124.9 (3)	124.8 (3)	123.6 (3)	123.5 (3)	125.1 (4)
O1—C9—O2	122.4 (2)	122.6 (3)	123.6 (3)	123.0 (3)	123.1 (3)
C31—C4—Cl	119.7 (2)				
C5—C4—Cl	118.6 (2)				
C4—C5—Cl		119.3 (2)			
C6—C5—Cl		118.0 (3)			
C5—C6—Cl			118.9 (3)	118.9 (3)	117.7 (3)
C7—C6—Cl			119.1 (3)	118.7 (3)	119.7 (3)
C6—C7—Cl					121.9 (3)
C71—C7—Cl					119.6 (3)
C4—C5—Br					
C6—C5—Br					119.2 (2)
					116.9 (2)

Table 5. Selected torsion angles (°) for monohalogenated indole-3-acetic acids

	4-Cl-IAA	5-Cl-IAA	6-Cl-IAA	7-Cl-IAA	5-Br-IAA
			A	B	C
T1* C2—C3—C8—C9	100.4 (4)	93.2 (4)	97.5 (5)	-54.5 (5)	100.1 (5)
C31—C3—C8—C9	-79.1 (4)	-82.3 (4)	-83.4 (5)	128.6 (4)	-83.9 (5)
C3—C8—C9—O1	179.4 (3)	176.3 (3)	-167.6 (3)	149.2 (3)	-172.2 (3)
T2* C3—C8—C9—O2	-2.5 (5)	-5.2 (5)	13.2 (6)	-32.8 (5)	8.1 (6)

*Labels used in computational chemistry procedures.

(Kojić-Prodić, Puntarec & Nigović, to be published; Chandrasekhar & Raghunathan, 1982) revealed the same effects, respectively. The values from low- and room-temperature experiments are, respectively: C6—C7

1.378 (3), 1.373 (5) Å and C6—C7—C71 117.4 (2), 117.2 (3)°. Inspection of the Cambridge Structural Database (1994) yielded 412 structures containing an indole moiety, of which 374 with *R* values smaller

than 0.07 were selected for statistical analysis by *GSTAT89* (Motherwell, Murray-Rust, Raftery, Allen & Doyle, 1989). Arithmetic means calculated from the selected data are 1.37 (1) Å for the length of the C6—C7 bond and 117.2 (8)° for the C6—C7—C71 angle. It is evident, therefore, that these changes from the

expected 120° have not been introduced by halogenation of the system, but rather are characteristics of the indole moiety. Departure of halogen atoms from the best least-squares plane of the indole has been observed and the largest effect is encountered in position 5 [0.115 (7) Å for 5-Cl-IAA and 0.119 (3) Å for 5-Br-IAA].

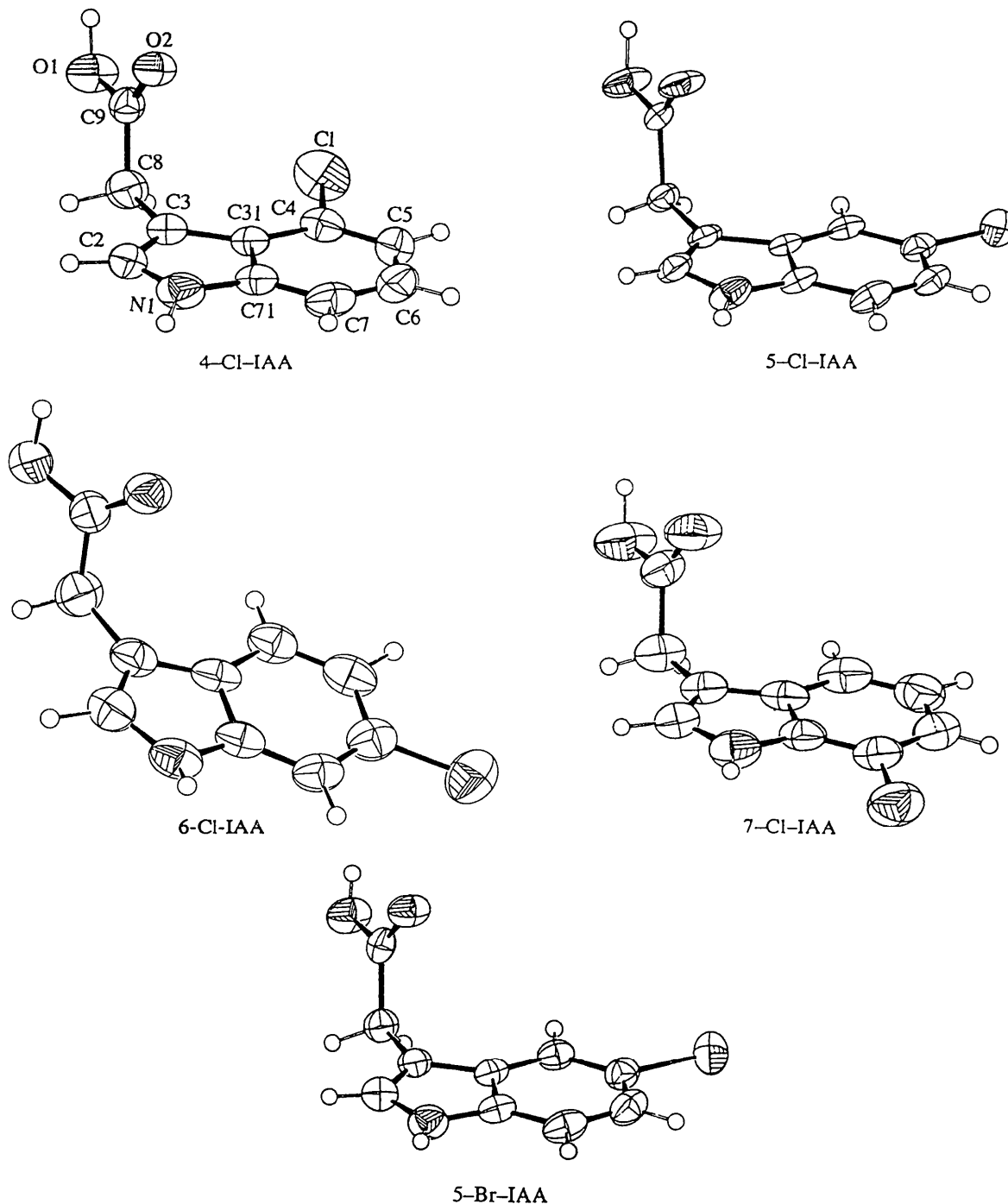


Fig. 1. Molecular structures (*ORTEP*) of monohalogenated indole-3-acetic acids. Atom numbering is shown for 4-Cl-IAA. The thermal ellipsoids are scaled at the 30% probability. In the case of 6-Cl-IAA, conformer *A* is displayed.

Table 6. Hydrogen bonds, C—H···O and N—H···C (phenyl) contacts in the structures of monohalogenated indole-3-acetic acids

Compound		D—H···A (Å)	D—H (Å)	H···A (Å)	D—H···A (°)	Space group
4-Cl-IAA	O1—H···O2 ⁱ	2.677 (3)	0.98 (5)	1.71 (4)	174 (4)	<i>P2₁/c</i>
	N1—H···O2 ⁱⁱ	2.965 (4)	1.01 (3)	1.96 (3)	170 (3)	
5-Cl-IAA	O1—H···O2 ⁱⁱⁱ	2.704 (3)	0.99 (5)	1.73 (6)	170 (5)	<i>P2₁/c</i>
	C2—H···O2 ⁱⁱ	3.335 (5)	0.93 (3)	2.45 (3)	161 (3)	
	N1—H···C4 ⁱⁱ	3.412 (4)	1.009	2.426	165 (3)	
	N1—H···C5 ⁱⁱ	3.449 (4)	1.009	2.553	147 (3)	
6-Cl-IAA*	(A)O1—H···O2 ^{iv} (A)	2.649 (4)	0.98 (2)	1.67 (2)	174 (3)	<i>Pbca</i>
	(B)O1—H···O2 ^v (C)	2.669 (4)	0.98 (3)	1.69 (3)	175 (3)	
	(C)O1—H···O2 ^v (B)	2.66 (4)	0.98 (2)	1.68 (2)	173 (3)	
	(B)N1—H···O2 ^v (B)	2.975 (5)	1.01 (4)	2.23 (4)	130 (3)	
	(C)N1—H···O2 ^{iv} (C)	3.155 (5)	1.01 (5)	2.54 (4)	119 (3)	
	O1—H···O2 ^{vi}	2.652 (4)	0.98 (4)	1.67 (4)	179 (4)	
7-Cl-IAA	C2—H···O2 ^{vi}	3.428 (5)	1.03 (3)	2.40 (3)	175 (2)	<i>P2₁/c</i>
	N1—H···C5 ^{vi}	3.369 (5)	1.009	2.395	162 (2)	
	O1—H···O2 ^{vii}	2.685 (2)	0.983 (7)	1.708 (7)	172.1 (7)	
5-Br-IAA	N1—H···O2 ^{viii}	3.174 (2)	0.931 (8)	2.279 (8)	161.0 (5)	<i>P1̄</i>

Symmetry codes: (i) $3-x, -y, 2-z$; (ii) $x, \frac{1}{2}-y, z-\frac{1}{2}$; (iii) $-x, 1-y, -z$; (iv) $-x, -y, -z$; (v) $x, y, z-1$; (vi) $x, \frac{3}{2}-y, \frac{1}{2}+z$; (vii) $-x, 2-y, -z$; (viii) $-x, 2-y, 2-z$; (ix) $-1-x, 1-y, 2-z$. * Three crystallographically independent molecules (A, B and C).

The overall conformation of the molecules is described with only two torsion angles (Table 5). The C2—C3—C8—C9 angle (*T1*) defines the relative orientations of a side chain towards the indole plane. The orientation of the carboxylic group is given by the C3—C8—C9—O2 angle (*T2*). In the crystal structures of the five compounds studied, regardless of the site of substitution and the size of the halogen atom, a side chain is close to being perpendicular to the indole plane. The only exception is one of the three conformers of 6-Cl-IAA having a (–)-synclinal conformation (Klyne & Prelog, 1961) about the C3—C8 bond (Table 5). The values of the C2—C3—C8—C9 torsion angle range from 93.2 (4) to 105.7 (5)° (Table 5). The conformation about the C8—C9 bond is (±)-synperiplanar; the values of the C3—C8—C9—O2 torsion angle are in the range

–32.8 (5)–13.2 (6)° (Table 5). The dihedral angles, between the planes of the carboxylic and indole residues, are in the range from 72.0 (2) (for 6-Cl-IAA, molecule B) to 88.9 (1)° (for 5-Cl-IAA). Thus, the plane of the carboxylic group is close to perpendicular to the C8—C9 bond.

4. Crystal packing

In the crystal structures of monohalogenated IAA's there are two chemically distinct hydrogen bonds acting between: (a) carboxylic groups, O1—H···O2, and (b) indole and carboxylic groups, N1—H···O2 (Table 6). The general pattern observed in all structures studied shows dimers formed around the inversion centers via O—H···O hydrogen bonds of the carboxylic groups (Figs. 2 and 3). There are two essentially different

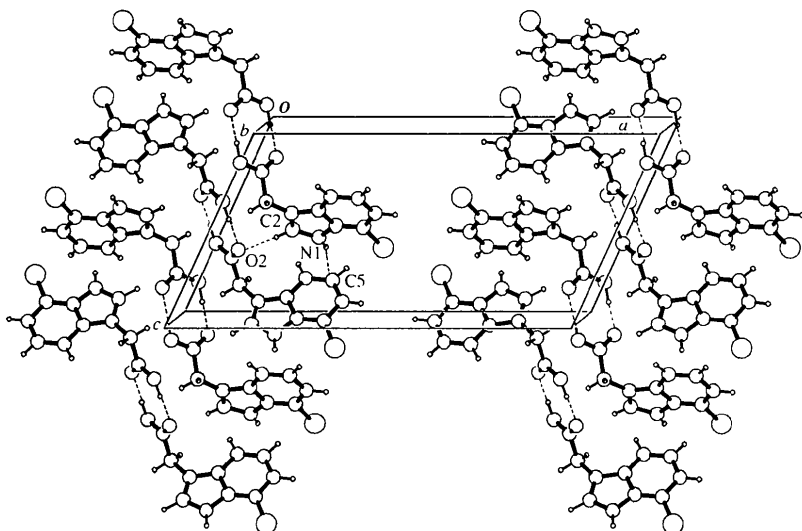


Fig. 2. Crystal packing of 7-Cl-IAA with O—H···O hydrogen bonds which create dimers around the inversion centers. The intermolecular contacts C2—H···O2 and N1—H···C5 are shown on a single pair of molecules.

packing arrangements, characterized by O—H···O dimers only and those with both types of hydrogen bonds O—H···O and N—H···O. The particular hydrogen-bond pattern is not space-group dependent. The compounds 4-Cl-IAA, 5-Cl-IAA and 7-Cl-IAA all crystallize in the space groups $P2_1/c$, but with two different patterns. The crystal structures of 5-Cl-IAA and 7-Cl-IAA revealed only the dimers hydrogen bonded *via* carboxylic groups, which are also present in a free hormone, IAA (Chandrasekhar & Raghunathan, 1982) and many organic acids (Cambridge Structural Database, 1994), as well as in *n*-alkyl-substituted IAA's (Kojić-Prodić, Nigović, Horvatić *et al.*, 1991) and achiral amino acid conjugates of IAA (Kojić-Prodić, Nigović, Tomić *et al.*, 1991). The packing pattern, which includes hydrogen-bonded dimers connected by hydrogen bonds N—H···O into the infinite chains was observed in the crystal structures of 4-Cl-IAA, 6-Cl-IAA and also in the structure of 5-Br-IAA (Table 6).

In addition to the classical type of hydrogen bonds detected in the structures studied, weak C—H···O [4.19–8.37 kJ mol⁻¹ (Desiraju, 1991)] and N—H···C [(phenyl) 8.37–16.75 kJ mol⁻¹ (Perutz, 1993)] interactions were observed; they are present in the crystal structures lacking N—H···O hydrogen bonds. In the crystal structures of 5-Cl-IAA and 7-Cl-IAA C—H···O intermolecular interactions, between the Csp^2 atom of the pyrrole ring and C=O of the carboxylic group, are present. The geometry observed (Table 6) is in agreement with the criteria described by Taylor & Kennard (1982), Berkovitch-Yellin &

Leiserowitz (1984) and Desiraju (1991). The occurrence of C—H···O interactions in the auxin derivatives and analogs was discussed recently by Kojić-Prodić, Kroon & Puntarec (1994). The N—H···phenyl interactions contribute to the packing of 5-Cl-IAA and 7-Cl-IAA; N1—H points to the phenyl edge C4—C5 (5-Cl-IAA) or to a single atom of the phenyl ring, C5 (7-Cl-IAA; Table 6). The N—H···C (phenyl) interaction might be important for substrate binding to the auxin-binding protein (or a receptor). Both, indole and nonindole auxins contain the aromatic nucleus which can interact with the auxin-binding protein active site (Edgerton, Tropsha & Jones, 1994). The first evidence of the acceptor function of the aromatic ring with regard to hydrogen bonds was given by Klemperer, Cronyn, Maki & Pimentel (1954). The energetical and geometrical criteria were discussed by Levitt & Perutz (1988). The stabilizing role in the structure of α -helices of proteins has been recognized (Perutz, 1993; Hunter, 1993). A somewhat different point was given by Mitchell, Nandi, McDonald, Thornton & Price (1994). These authors detected N—H···C hydrogen bonds, but found them to be rare and not stable enough to represent a significant contribution to protein stability. However, they do not deny their contribution in the context of molecular recognition. Evidence for N—H···C hydrogen bonding in crystalline alkynes, alkenes and aromatics (Viswamitra, Radhakrishnan, Bandekar & Desiraju, 1993) contributes to the knowledge of this unusual interaction. To reach consistent knowledge on this topic more examples should be studied.

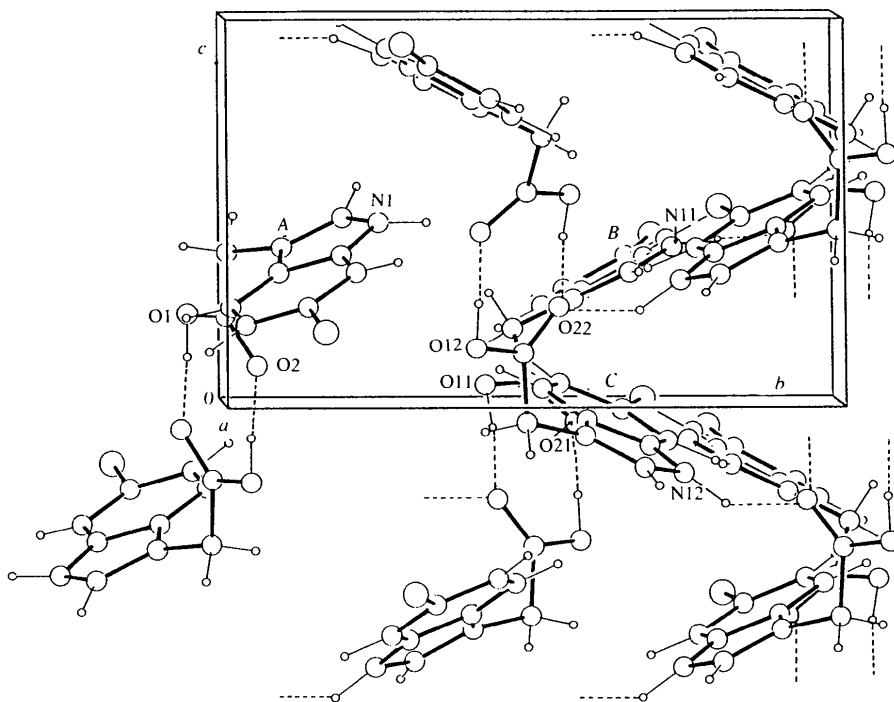


Fig. 3. Crystal packing of 6-Cl-IAA with three crystallographically independent molecules (*A*, *B* and *C*) connected by hydrogen bonds O1—H···O2 and N1—H···O2. For the sake of clarity, a single layer along $\frac{1}{2}a$ is only shown.

Table 7. Conformation analysis of halogenated IAA about C3—C8 and C8—C9 bonds

Calculations were performed by DISCOVER (CVFF).

Torsion angles (°)* refer to C2—C3—C8—C9, first entry; C3—C8—C9—O2, second entry.

	4-Cl-IAA		5-Cl-IAA		6-Cl-IAA		7-Cl-IAA		5-Br-IAA	
X-ray analysis	100.4	-2.5	93.2	-5.2	100.1	8.1‡	105.7	-4.1	100.7	3.0
Molecular mechanics										
Input atomic coordinates: X-ray data										
(a) Molecule optimized <i>in vacuo</i> without constraint	84	-106	-94	112	96	113	101	106	100	94
(b) Molecule optimized <i>in vacuo</i> with tethering† to the conformation found in the crystal	99	-4	-93	6	94	17	103	-3	99	3
ΔE [(between (a) and (b): $E_b - E_a$] (kJ mol ⁻¹)	9.2		10.5		11.3		10.9		9.6	

*The molecules studied are achiral and the sign of the torsion angles is relevant in the comparison of relative orientations of the carboxylic group and indole moiety only. † A penalty function is used which keeps the atoms close to their initial positions. ‡ Molecule C.

5. Molecular mechanics and molecular dynamics

In order to explore the conformational flexibility of monohalogenated IAA's that may be related to biological activity, molecular mechanics and dynamics simulations were carried out using DISCOVER (Biosym Technologies, 1994), Version 2.9.5, with the CVFF (Hagler, Dauber & Lifson, 1979) and CFF91 (Maple, Thacher, Dinur & Hagler, 1990) versions of the force fields. The results obtained with both force fields are in accordance with the prediction of energy minima.

Complete energy optimization of the crystallographically determined structures was performed *in vacuo* (CVFF) for each molecule: (a) without any constraint and (b) with tethering conformation to the starting one; a penalty function was used which kept the atoms close to their initial positions. The results are summarized in Table 7. The synperiplanar orientation about the C8—C9 bond found in the crystal changed during the optimization to anticlinal (+ or -; Table 7). According to the molecular mechanics results, the conformations found in the crystal structures are not global minima.

Molecular mechanics calculations were extended to molecular dynamics simulations *in vacuo* in order to explore the conformational space more thoroughly. In these procedures, the regions of low potential energies and possible conformational transitions were localized. The rotations about the pair of relevant bonds (C3—C9), in steps of 15° (CVFF), performed for the compounds

4-Cl-IAA, 5-Cl-IAA, 6-Cl-IAA, 7-Cl-IAA and 5-Br-IAA, finished with very similar results. Thus, the energy profile as a function of two characteristic torsion angles (T_1 , T_2) is shown for 5-Br-IAA only (Fig. 4). The rotations were followed by molecular dynamics simulations *in vacuo* for 250 ps over a range of temperatures (300–450 K). The results obtained for 4-Cl-IAA, superimposed on the contour graphs obtained by rotations, are given in Fig. 5. The most populated regions in two-dimensional space are: $T_1 = 90 \pm 30$, $T_2 = 90 \pm 30$ and $T_1 = 90 \pm 30$, $T_2 = -90 \pm 30^\circ$ (the molecule is achiral and conformations $T_1 = -90 \pm 30$, $T_2 = -90 \pm 30$ and $T_1 = -90 \pm 3$, $T_2 = -90 \pm 30$, $T_2 = 90 \pm 30^\circ$ are the mirror images of the previous ones). Transitions between these regions are frequent during simulations *in vacuo* and occur mostly through the saddle points $T_1 \sim 90$, $T_2 \sim 0$ and $T_1 \sim 0$, $T_2 \sim 90^\circ$ (Fig. 5).

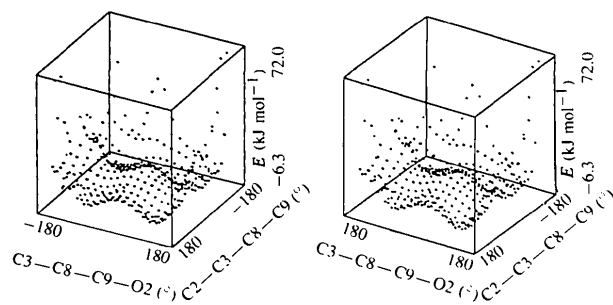


Fig. 4. Stereo diagram of conformational energy (kJ mol⁻¹) distribution for 5-Br-IAA as a function of two characteristic torsion angles (T_1 and T_2).

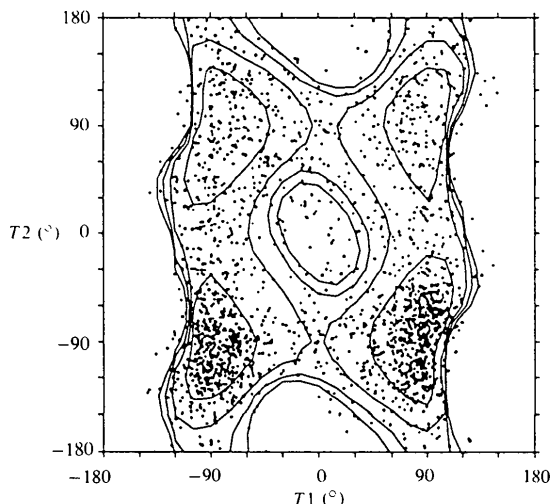


Fig. 5. Molecular dynamics simulation for 4-Cl-IAA *in vacuo* at elevated temperatures (300–450 K) over 250 ps. The values of torsion angles (°) T_1 and T_2 , obtained during the simulations, are superimposed on the contour graph (obtained by rotations about pairs of the bonds C3—C8 and C8—C9). The contour lines are drawn at an interval of 8.37 kJ mol⁻¹. The locations of energy minima in contour graphs coincide with the mostly populated conformations (high density of dots in molecular dynamics simulations).

To simulate natural conditions and to evaluate the influence of solvent on the conformational behavior of the compound, molecular dynamics simulations were performed in water. The simulations were carried out by *DISCOVER* (Biosym Technologies, 1994) with *CVFF* using periodic boundary conditions. The explicit image model applying two values of the cut-off parameters (13 and 16 Å) was used with a cube ($a = 15$ Å) as a unit cell. Before simulations, the systems were subjected to steepest descent minimization to relieve unfavorable interactions. After 5 ps of equilibration, the simulations over 250 ps were carried out. Water exerts a damping force on the conformational changes, especially when a relatively stable conformation is achieved. To overcome this effect and to sample larger conformational space, the simulations were performed at elevated temperatures (300–450 K). The results obtained are similar for all the compounds studied and the graphic presentation is given only for 4-Cl-IAA (Fig. 6). The most frequent conformations of monohalogenated IAA's detected during the simulations in water are similar to those found *in vacuo*: with $T1 \sim 90$ (± 30) and $T2 \sim \pm 90^\circ$ (± 30). Although the dispersion of conformations in the two-dimensional torsional space ($T1$ and $T2$) is not as large as *in vacuo*, the region about the saddle point $T1 \sim 90$ (± 30) and $T2 \sim 0^\circ$ (± 30) is more populated in water than *in vacuo*. In the crystal the molecule is in this type of conformation ($T1 \sim 90$ and $T2 \sim 0^\circ$, Table 6). In the polar environment, as in water and in the crystal, this very conformation is stabilized by intermolecular hydrogen bonds $O-H \cdots O$ (Table 6). The conformational analysis in *MM3(92)* force field, performed using

the drive option (Kojić-Prodić, Banić, Kroon-Batenburg & Kroon, 1994) for 4-Cl-IAA, besides the minima discussed before, revealed the minimum $T1 \sim 0$ and $T2 \sim 90^\circ$. In all the force fields used molecular mechanics calculations failed to predict planar ($T1 \sim 0$ and $T2 \sim 0^\circ$) and conformations found in the crystals ($T1 \sim 90$ and $T2 \sim 0^\circ$, Table 6) as minima. According to the preliminary *ab initio* results on 4-Cl-IAA (Ramek, Tomić & Kojić-Projić, unpublished results), its minima are: the planar conformation ($T1 \sim 0$ and $T2 \sim 0^\circ$), the conformations with $T1 \sim 90^\circ$, $T2$ synperiplanar (similar to the conformation determined in crystal) and $T1 \sim 90^\circ$, $T2$ antiperiplanar. The results obtained by systematic *ab initio* SCF conformational analysis on indole-3-acetic acid (Ramek, Tomić & Kojić-Prodić, 1995) considerably differ from those of molecular mechanics calculations in various force fields [*MM2(87)*, *MM3*, *CVFF*, *CFF91* and *TRIPOS*; Tomić, 1993]. Molecular mechanics were unable to locate two of the four minima obtained by *ab initio* calculations. In order to detect possible conformers and to see their relative energetic stability, *ab initio* SCF conformational analysis of monohalogenated IAA derivatives is needed.

However, all computational chemistry methods used, including the *ab initio* SCF approach, revealed energy differences among the following conformations $T1 \sim 0$, $T2 \sim 0$, $T1 \sim 90$, $T2 \sim 0$, $T1 \sim 90$, $T2 \sim \pm 90^\circ$ of IAA and its monohalogenated species within the limits acceptable from the point of *QSAR* philosophy (Kubinyi, 1993; Table 7, Figs. 4, 5 and 6). Therefore, all are potentially active conformations. The slightly higher energy of some of these conformations can be easily compensated by the stabilization of the whole system (substrate + ABP) during binding.

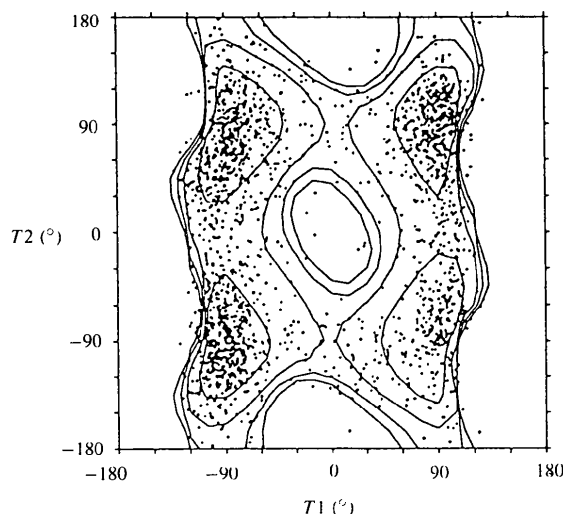


Fig. 6. Molecular dynamics simulation for 4-Cl-IAA in water at elevated temperatures (300–450 K) over 250 ps. The values of the torsion angles ($^\circ$) $T1$ and $T2$, obtained during the simulations, are superimposed on the contour graph (the energy intervals are 8.37 kJ mol^{-1}). In aqueous medium the number of conformational changes is somewhat reduced.

6. Discussion and conclusions

Hormonal activity in higher plants is a very complicated mechanism related to a number of parameters, *e.g.* receptor affinity towards the auxins, metabolic stability, distribution of hormone in particular tissues, concentration of hormone at the receptor binding site and many other physicochemical parameters. Several auxin binding proteins (ABP) were characterized (Jones, 1990, 1994; Klämbt, 1990; Brown & Jones, 1994), but none have been identified as the auxin receptor(s). Therefore, the recognition of receptor(s) and the mode of hormone binding at the active site remains unknown. Even in the case of having a receptor identified, the precise structural information about small active molecules is a prerequisite for receptor–auxin binding studies. In the molecular recognition approach we examined characteristic features of biologically active monohalogenated compounds. Monohalogenation of indole-3-acetic acids develops auxin activity, particularly 4-Cl-IAA which is *ca* ten times more active than IAA itself (Fig. 7).

Biological activity is related to the type of halogen atom and the site of substitution. Bioassays performed in the *Avena mesocotyl* tests revealed the ratio of activity IAA:4-Cl-IAA:5-Cl-IAA:5-Br-IAA:6-Cl-IAA:7-Cl-IAA = 1:10:3.3:0.3:19:0.13 (Böttger, Engvild & Soll, 1978). *Zea mays* mutant tests based on the measurements of increased length of coleoptiles, standardized against IAA (relative activity), showed that 4- and 6-Cl-IAA are more active than IAA (Klämbt, 1994, private information). However, 5-Cl-IAA is somewhat less active than IAA, whereas 7-Cl-IAA is of low activity. This type of result is very much dependent on plant species, the tissue used and also on the experimental conditions. However, the general trend on the activity can be learnt. Instead of the auxin-induced growth test, most probably, more complicated but more reliable auxin-binding (to protein) constants should be used for judging structure-activity correlations. The size of the halogen atoms, in this case Cl and Br, affects the activity of the compounds studied (Table 7). Their almost equal Hammett sigma values ($\sigma_{\text{meta}} \sim 0.4$, $\sigma_{\text{para}} \sim 0.2$; Jaffe, 1953) are connected with their similar lipophilicity. The influence of the site substitution on the activity was also observed on mono- and dichloro-IAA's: the reduction of physiological effects for various sites follows the order $4 > 6 > 2 > 5 > 7$ (Porter & Thimann, 1965). However, these findings do not correlate with the values of partition coefficients determined in the *n*-octanol:water system (Katekar & Geissler, 1982). It is not possible to state simple, direct correlation between auxin activity and the lipophilicity of these compounds. More lipophilic dihalogenated IAA's are weak auxins or even antiauxins (Böttger, Engvild & Soll, 1978). Besides these complicated relationships, differences in the structure-activity of halogenated auxins on various

plant species (e.g. pea and wheat) were observed (Katekar & Geissler, 1983). They might be explained by different binding modes or even different receptor structures.

However, the conformational space of the hormone and its analogs should be examined. The results of X-ray structure analysis, molecular mechanics calculations, molecular dynamics simulations and *ab initio* SCF calculations on monohalogenated IAA's and IAA itself revealed the variety of conformations that should be included in a QSAR analysis. Molecular mechanics calculations have detected some, but not all, minima of IAA and 4-Cl-IAA proven by *ab initio* SCF calculations and its results should be taken with caution. Nevertheless, energy differences, determined by molecular mechanics calculations (CVFF), between conformations with various orientations of the carboxylic group (T_2 : $0-180^\circ$) and the side chain (T_1 : $0-90^\circ$) are such that all conformers from the regions specified should be considered in QSAR analysis even if *ab initio* results would be unknown. The influence of the conformation of the side chain on biological activity was proposed by Veldstra (1944) and extended by Kaethner (1977), who postulated free rotation of a side chain at two characteristic positions: (a) *recognition conformation*, with the COOH moiety coplanar to, and (b) *modulation conformation* with that group perpendicular to the indole nucleus. *Ab initio* SCF calculations on IAA (Ramek, Tomić & Kojić-Prodić 1995) and rotational coherence spectroscopy (Connell, Corcoran, Joireman & Felker, 1990) detected a planar molecule. Edgerton, Tropsha & Jones (1994) have not considered these two conformations, invoked by Kaethner (1977) and Katekar (1979), to be essential for binding. According to them, the phytophoric conformation is one with a side chain perpendicular to the aromatic plane ($T_1 \sim 90^\circ$) and carboxylic acid oxygens positioned directly astride the ring system.

This work was partly supported by the Ministry of Science and Technology, Republic of Croatia, grant no. 1-07-179 and NSF, no. JF831. The authors thank Dr W. L. Duax, Hauptman-Woodward Medical Research Institute, Buffalo, USA, and Dr P. B. van Eijck, Bijvoet Centre for Biomolecular Research, University of Utrecht, The Netherlands, for their criticism and suggestions during these studies. The results of bioassays performed on *Zea mays* mutant for the compounds studied were kindly provided by Professor Dr D. Klämbt, Botanisches Institut und Botanischer Garten, Rheinische Friedrich-Wilhelms Universität, Bonn, Germany.

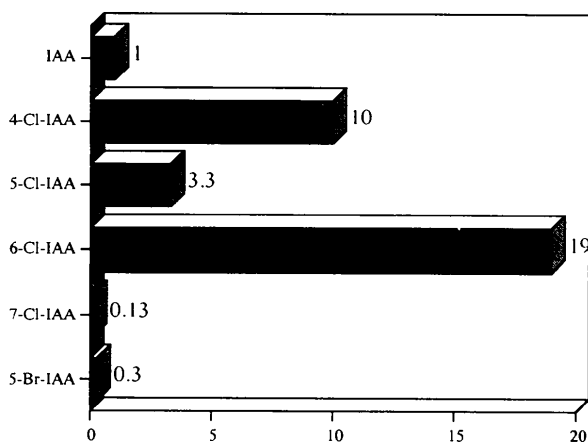


Fig. 7. Relative activity of monohalogenated indole-3-acetic acids according to Böttger, Engvild & Soll (1978); it is expressed as the concentration of IAA ($7.5 \times 10^{-7} \text{ mol l}^{-1}$) needed to give half the maximum elongation, divided by the concentration of the substituted IAA giving the same elongation.

References

- B. A. Frenz & Associates, Inc. (1982). *SDP Structure Determination Package*. College Station, Texas, USA.

- Baldi, B. G., Slovin, J. P. & Cohen, J. D. (1985). *J. Labelled Compd. Radiopharm.* **22**(3), 279–285.
- Berkovitch-Yellin, Z. & Leiserowitz, L. (1984). *Acta Cryst.* **B40**, 159–165.
- Biosym Technologies (1994). *DISCOVER*. Version 2.9.5. *INSIGHTII*. Version 2.3.0. Biosym Technologies, 1065 Barnes Canyon Road, San Diego, CA 92121, USA.
- Böttger, M., Engvild, K. C. & Soll, H. (1978). *Planta*, **140**, 89–92.
- Brown, J. C. & Jones, A. M. (1994). *J. Biol. Chem.* **269**, 21136–21140.
- Cambridge Structural Database (1994). Version 5.07. Cambridge Crystallographic Data Centre, 12 Union Road, Cambridge, England.
- Chandrasekhar, K. & Raghunathan, S. (1982). *Acta Cryst.* **B38**, 2534–2535.
- Connell, L. L., Corcoran, T. C., Joireman, P. W. & Felker, P. M. (1990). *Chem. Phys. Lett.* **166**, 510–516.
- Cramer III, R. D., Scott, A., DePriest, S. A., Patterson, D. E. & Hecht, P. (1993). *3D QSAR in Drug Design Theory, Methods and Applications*, edited by H. Kubinyi, pp. 443–485. Leiden: ESCOM.
- Desiraju, G. R. (1991). *Acc. Chem. Res.* **24**, 290–296.
- Edgerton, M. D., Tropsha, A. & Jones, A. M. (1994). *Phytochemistry*, **35**, 1111–1123.
- Engvild, K. C., Egsgaard, H. & Larsen, E. (1978). *Physiol. Plant.* **42**, 365–368.
- Enraf-Nonius (1989). *CAD-4 Software*. Version 5.0. Enraf-Nonius, Delft, The Netherlands.
- Ernsten, A. & Sandberg, G. (1986). *Physiol. Plant.* **68**, 511–518.
- Hagler, A. T., Dauber, P. & Lifson, S. (1979). *J. Am. Chem. Soc.* **101**, 5131–5141.
- Hofinger, M. & Büttger, M. (1979). *Phytochemistry*, **18**, 653–654.
- Hunter, C. A. (1993). *Philos. Trans. R. Soc. London Ser. A*, **345**, 77–85.
- Jaffe, H. H. (1953). *Chem. Rev.* **53**, 191–261.
- Johnson, C. K. (1976). *ORTEPII*. Report ORNL-5138. Oak Ridge National Laboratory, Tennessee, USA.
- Jones, A. M. (1990). *Physiol. Plant.* **80**, 154–158.
- Jones, A. M. (1994). *Annu. Rev. Plant Physiol. Plant Mol. Biol.* **45**, 393–420.
- Kaethner, T. M. (1977). *Nature (London)*, **267**, 19–23.
- Katekar, G. F. (1979). *Phytochemistry*, **18**, 223–233.
- Katekar, G. F. & Geissler, A. E. (1982). *Phytochemistry*, **21**, 257–260.
- Katekar, G. F. & Geissler, A. E. (1983). *Phytochemistry*, **22**, 27–31.
- Klämbt, D. (1990). *Plant Mol. Biol.* **14**, 1045–1050.
- Klemperer, W., Cronyn, M. W., Maki, A. M. & Pimentel, G. C. (1954). *J. Am. Chem. Soc.* **76**, 5846–5848.
- Klyne, W. & Prelog, V. (1960). *Experientia*, **16**(12), 521–568.
- Kojić-Prodić, B., Banić, Z., Kroon-Batenburg, L. & Kroon, J. (1994). 15th European Crystallographic Meeting, Dresden, 28 August–2 September, p. 483. München: Oldenburg-Verlag.
- Kojić-Prodić, B., Kroon, J. & Puntarec, V. (1994). *J. Mol. Struct.* **322**, 43–69.
- Kojić-Prodić, B., Nigović, B., Horvatić, D., Ružić-Toroš, Ž., Magnus, V., Duax, W. L., Stezowski, J. J. & Bresciani-Pahor, N. (1991). *Acta Cryst.* **B47**, 107–115.
- Kojić-Prodić, B., Nigović, B., Tomić, S., Ilić, N., Magnus, V., Konjević, R., Giba, Z. & Duax, W. L. (1991). *Acta Cryst.* **B47**, 1010–1019.
- Kubinyi, H. (1993). Editor. *3D QSAR in Drug Design Theory, Methods and Applications*. Leiden: ESCOM.
- Levitt, M. & Perutz, M. F. (1988). *J. Mol. Biol.* **201**, 751–754.
- Maple, J. R., Thacher, T. S., Dinur, U. & Hagler, A. T. (1990). *Chem. Des. Autom. News*, **5**, 5–10.
- Marumo, S., Abe, H., Hattori, H. & Munakata, K. (1968). *Agric. Biol. Chem.* **32**, 117–118.
- Marumo, S., Hattori, H. & Abe, H. (1971). *Analyt. Biochem.* **40**, 488–490.
- Marumo, S., Hattori, H., Abe, H. & Munakata, K. (1968). *Nature (London)*, **219**, 959–960.
- Mitchell, J. B. O., Nandi, C. L., McDonald, I. K., Thornton, J. M. & Price, S. L. (1994). *J. Mol. Biol.* **239**, 315–331.
- Motherwell, S., Murray-Rust, P., Raftery, J., Allen, F. & Doyle, M. (1989). *GSTAT89. Cambridge Structural Database Integrated Program for Molecular Geometry Parameter Calculations*. Cambridge Crystallographic Data Centre, 12 Union Road, Cambridge, England.
- Perutz, M. F. (1993). *Philos. Trans. R. Soc. London Ser. A*, **345**, 105–112.
- Porter, W. L. & Thimann, K. V. (1965). *Phytochemistry*, **4**, 229–243.
- Ramek, M., Tomić, S. & Kojić-Prodić, B. (1995). *Int. J. Quantum Chem.* In the press.
- Sheldrick, G. M. (1976). *SHELX76. Program for Crystal Structure Determination*. University of Cambridge, England.
- Sheldrick, G. M. (1985). *SHELXS86. Crystallographic Computing 3*, edited by G. M. Sheldrick, C. Krüger & R. Goddard, pp. 175–189. Oxford University Press.
- Spek, A. L. (1982). *The EUCLID Package. Computation Crystallography*, edited by D. Sayre, p. 528. Oxford: Clarendon Press.
- Spek, A. L. (1990). *Acta Cryst.* **A46**, C-34.
- Stenlid, G. & Engvild, K. C. (1987). *Physiol. Plant.* **70**, 109–113.
- Taylor, R. & Kennard, O. (1982). *J. Am. Chem. Soc.* **104**, 5063–5070.
- Tomić, S. (1993). Ph.D. Thesis. University of Zagreb, Zagreb.
- Veldstra, H. (1944). *Enzymologia*, **11**, 97–163.
- Viswamitra, M. A., Radhakrishnan, R., Bandekar, J. & Desiraju, G. R. (1993). *J. Am. Chem. Soc.* **115**, 4868–4869.